Green Energy & Environment

ISSN 2096-2797 E-ISSN 2468-0257 CN 10-1418/TK Volume 7, Issue 6 (2022.12)

Front Cover

See Liangliang Dong, Hongwei Fan, Hong Meng *et al.*,
Image reproduced by permission of Liangliang Dong,
Hongwei Fan, Hong Meng from
Green Energy & Environment

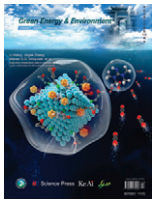

Back Cover

See Li Wang, Jinglai Zhang,
Mårten S.G. Ahlquist *et al.*,
Image reproduced by permission of Li Wang,
Jinglai Zhang, Mårten S.G. Ahlquist from
Green Energy & Environment

CONTENTS

The application of hydrogen spillover effect in hydrogen storage and catalysis was comprehensively summarized.

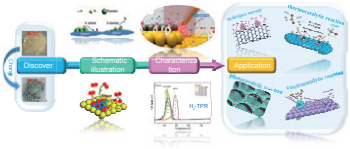

Research papers

Novel design and synthesis of 1D bamboo-like CNTs@Sn_4P_3@C coaxial nanotubes for long-term sodium ion storage

Novel bamboo-like carbon nanotubes@Sn_4P_3@carbon coaxial nanotubes are sucessfully prepared using a newly developed hydrothermal method followed by a phophidation process, which can serve as advanced anode with excellent reversible capacity and a long cycling in sodium ion storage.

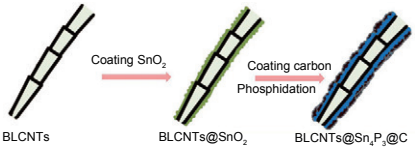

Poly(thiourea triethylene glycol) as a multifunctional binder for enhanced performance in lithium-sulfur batteries

Poly(thiourea triethylene glycol) PTTG polymer used as a lithium-sulfur battery (LSB) binder shows strong chemical interaction with soluble polysulfides. Sulfur-PTTG cathodes possess high electronic and ionic conductivity as well as robust mechanical properties to provide excellent LSB performance.

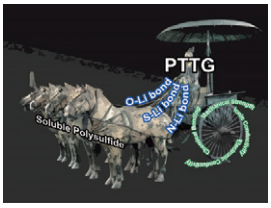

Deep eutectic solvent strategy enables an octahedral Ni–Co precursor for creating high-performance $NiCo_2O_4$ catalyst toward oxygen evolution reaction

An innovative DES strategy was proposed for synthesizing water-sensitive NiCo–NH_3 complex precursor, which was effectively converted into $NiCo_2O_4$ nanooctahedrons via thermal decomposition, realizing a high-performance OER electrocatalyst.

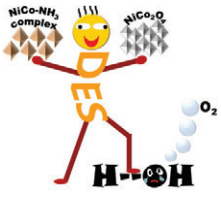

Engineered NiCo-LDH nanosheets- and $ZnFe_2O_4$ nanocubes-decorated carbon nanofiber bonded mats for high-rate asymmetric supercapacitors

The coreeshell NiCo-LDH nanosheet- and $ZnFe_2O_4$ nanocube-decorated carbon nanofiber composites with bonded network structure as cathode and anode electrode materials were prepared. The fabricated supercapacitor device delivered a specific capacitance of ~98 F g^{-1} at 1 A g^{-1} and excellent

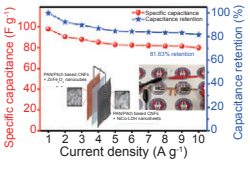

Here, we synthesized $Fe(acac)_3$/Bp-COF composite photocatalyst in one step under mild conditions. Compared with Bp-COF, composite photocatalyst has facile preparation and exhibits highly improved light absorbance and transformation of photogenerated electronehole pairs. The composite photocatalyst can efficiently convert benzyl alcohol into benzaldehyde under the condition of room temperature and air as oxidant without producing other by-products.

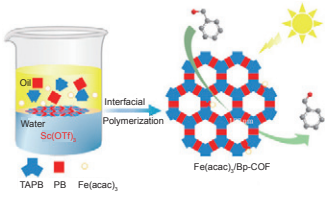

Manganese doping to boost the capacitance performance of hierarchical Co_9S_8@$Co(OH)_2$ nanosheet arrays

The introduction of Mg dopants endows tuned electronic structure of Co_9S_8@$Co(OH)_2$ nanosheets and enhanced interfacial activities as well as facilitated reaction kinetics, leading to ultrahigh capacity and outstanding long-term stability. The encouraging results might offer an effective strategy to optimize the electrodes for high-performance energy-storage devices.

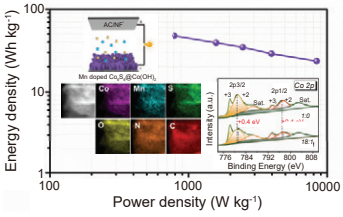

Disposal methods for used passenger car tires: One of the fastest growing solid wastes in China

Waste tire generation and disposal methods in China were investigated. Tire retreading and tire rubber reclaiming had no longer sufficient to recycle those waste tires. Pyrolysis technology is regarded as a promising way to solve this fast increasing solid wastes.

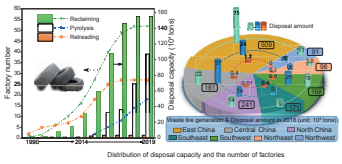

Biomass-based N doped carbon as metal-free catalyst for selective oxidation of D-xylose into D-xylonic acid

A defect-rich N doped carbon catalyst exhibits high catalytic activity for selective oxidation of D-xylose into D-xylonic acid. With graphitic N as the intrinsic active sites, D-xylonic acid yield of 57.4% could be obtained.

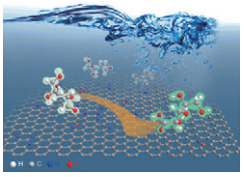

A new perspective on polyethylene-promoted lignin pyrolysis with mass transfer and radical explanation

Mass transfer and radical reactions together controlled the co-pyrolysis of lignin and PE. Good mass transfer in layered lignin/PE co-pyrolysis approach promoted the radical quenching reactions and favored the formation of lignin-derived phenols.

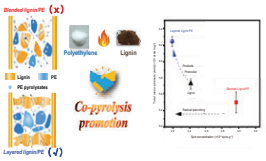

Dual-ionic imidazolium salts to promote synthesis of cyclic carbonates at atmospheric pressure

A novel dual-ionic imidazolium salt displays the excellent catalytic activity for cycloaddition of carbon dioxide and epoxides at ambient temperature and CO_2 pressure under solvent free conditions without any additional catalysts.

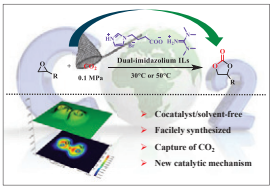

Enhanced catalytic conversion of polysulfides using high-percentage 1T-phase metallic WS_2 nanosheets for Li-S batteries

The conversion mechanism of S on the surface of 1T-WS_2 and 2H-WS_2 in Li-S battery.

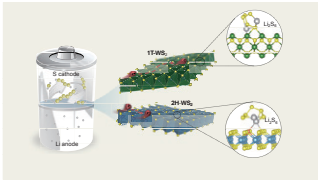

Pt-Pd bimetallic nanoparticles anchored on uniform mesoporous MnO_2 sphere as an advanced nanocatalyst for highly efficient toluene oxidation

Uniform mesoporous MnO_2 nanosphere-supported bimetallic Pt-Pd nanoparticles were successfully fabricated using hard templates for the total catalytic degradation of volatile organic compounds at low temperature. The introduction of mesopores into the MnO_2 support induces a large specific surface area and pore size, thus providing numerous accessible active sites and enhanced diffusion properties. Moreover, the addition of a secondary noble metal can adjust the O_{ads}/O_{latt} molar ratios, resulting in high catalytic activity.

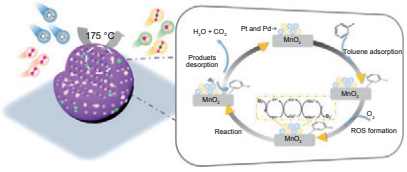

Green and selective hydrogenation of aromatic diamines over the nanosheet Ru/g–C_3N_4–H_2 catalyst prepared by ultrasonic assisted impregnation-deposition method

Nanosheet g-C_3N_4-H_2 was derived from thermal exfoliation of bulk g-C_3N_4 under hydrogen atmosphere, then a green catalyst with ultrafine Ru species supported on the nanosheet g-C_3N_4-H_2 was prepared by facile ultrasonic assisted impregnation-deposition method and the Ru/g-C_3N_4-H_2